

## 4-Iminooxazolidin-2-one as a bioisostere of the cyanohydrin moiety: inhibitors of enterovirus 71 3C protease

Yuying Ma, Chengyou Shang, Peng Yang, Linfeng Li,  
Yangyang Zhai, Zheng Yin, Binghe Wang, and Luqing Shang

*J. Med. Chem.*, **Just Accepted Manuscript** • DOI: 10.1021/acs.jmedchem.8b01335 • Publication Date (Web): 26 Oct 2018

Downloaded from <http://pubs.acs.org> on October 26, 2018

### Just Accepted

“Just Accepted” manuscripts have been peer-reviewed and accepted for publication. They are posted online prior to technical editing, formatting for publication and author proofing. The American Chemical Society provides “Just Accepted” as a service to the research community to expedite the dissemination of scientific material as soon as possible after acceptance. “Just Accepted” manuscripts appear in full in PDF format accompanied by an HTML abstract. “Just Accepted” manuscripts have been fully peer reviewed, but should not be considered the official version of record. They are citable by the Digital Object Identifier (DOI®). “Just Accepted” is an optional service offered to authors. Therefore, the “Just Accepted” Web site may not include all articles that will be published in the journal. After a manuscript is technically edited and formatted, it will be removed from the “Just Accepted” Web site and published as an ASAP article. Note that technical editing may introduce minor changes to the manuscript text and/or graphics which could affect content, and all legal disclaimers and ethical guidelines that apply to the journal pertain. ACS cannot be held responsible for errors or consequences arising from the use of information contained in these “Just Accepted” manuscripts.

# 4-Iminooxazolidin-2-one as a bioisostere of the cyanohydrin moiety: inhibitors of enterovirus 71 3C protease

Yuying Ma,<sup>†</sup> Chengyou Shang,<sup>†</sup> Peng Yang,<sup>†</sup> Linfeng Li,<sup>‡</sup> Yangyang Zhai,<sup>§</sup> Zheng Yin,<sup>†</sup> Binghe Wang,<sup>\*,||</sup> and Luqing Shang<sup>\*,†</sup>

<sup>†</sup>College of Pharmacy, State Key Laboratory of Medicinal Chemical Biology and Tianjin Key Laboratory of Molecular Drug Research, Nankai University, Tianjin, 300350, China

<sup>‡</sup>Department of Biochemistry and Biophysics, Texas A&M University, College Station, TX 77843, United States

<sup>§</sup>Medical College, Henan Polytechnic University, Jiaozuo, 454000, China

<sup>||</sup>Department of Chemistry, Georgia State University, Atlanta, GA 30303, United States

*Supporting Information Placeholder*

**ABSTRACT:** A recently reported potent inhibitor of enterovirus 71 3C protease, **(R)-1**, was found to have stability and potential toxicity issues due to the presence of a cyanohydrin moiety. Modifying the labile cyanohydrin moiety, by serendipity, led to the discovery of 4-iminooxazolidin-2-one-based inhibitors **4e** and **4g** with potent inhibitory activity and significantly improved stability. *In vivo* pharmacokinetic studies of **4e** also demonstrated high plasma exposure and moderate half-life. These compounds have shown potential of becoming anti-EV71 drug candidates.

## INTRODUCTION

Hand, foot and mouth disease (HFMD), primarily caused by coxsackievirus A16 (CVA16) and enterovirus 71 (EV71), is a highly contagious infection that usually causes mild symptoms such as fever and malaise.<sup>1</sup> However, EV71-infected cases tend to be more severe than the CVA16-infected cases, and could have neurological or cardiopulmonary complications.<sup>2</sup> Although two inactivated EV71 vaccines have been approved in China for HFMD prevention, the development of antiviral drugs is still of great urgency since no specific clinical treatment is available.<sup>3</sup>

The EV71 genome encodes a large polyprotein precursor that is subsequently processed into four structural proteins (VP1-VP4) and seven non-structural proteins (2A-2C and 3A-3D).<sup>4</sup> Viral 3C protein (3C<sup>pro</sup>) is a cysteine protease with chymotrypsin-like specificity, and is critical for most of the cleavage events in polyprotein processing. In addition to acting on virus itself, 3C<sup>pro</sup> can hamper host cell function in different ways such as interfering with host gene expression or disturbing the innate immune system.<sup>5</sup> Therefore, the importance of 3C<sup>pro</sup> in the viral life cycle makes it an attractive target for anti-EV71 drug discovery.

The approach of structure-based design has generated quite a few promising inhibitors of EV71 3C<sup>pro</sup>. Rupintrivir, originally developed as an inhibitor of human rhinovirus (HRV) protease,<sup>6</sup> can effectively inhibit EV71 replication and is deemed an archetype in the design of peptidomimetic inhibitor of EV71 3C<sup>pro</sup>.<sup>7</sup> Based on the crystal structure of EV71 3C<sup>pro</sup>-rupintrivir complex,<sup>8</sup> our

group has long been committed to the development of 3C<sup>pro</sup> inhibitors with improved potency and drug-like properties.<sup>9</sup> In 2015, **(R)-1** was reported as a novel inhibitor, consisting of a fine-tuned peptidyl scaffold and a cyanohydrin warhead.<sup>10</sup> Despite its significant improvement in both potency and selectivity for cysteine protease (EV71 3C<sup>pro</sup>, SARS-CoV M<sup>pro</sup>) over serine protease (human neutrophil elastase, human trypsin etc.), the presence of a cyanohydrin group gives rise to stability and potential toxicity issues.<sup>11</sup>

In this work, we undertook an effort to optimize **(R)-1** for improved stability and pharmacokinetic properties. Very excitingly, after several rounds of modification, we identified a 4-iminooxazolidin-2-one moiety that serves as an excellent replacement of the labile cyanohydrin group, allowing for maintaining comparable potency as **(R)-1**. Thus, 4-iminooxazolidin-2-one does appear to serve as a nonclassical bioisostere of protected cyanohydrin. Such a discovery solved one critical problem with the original structural scaffold of this class of otherwise very promising anti-EV71 compounds. These findings also have opened doors for further studies to examine whether the 4-iminooxazolidin-2-one moiety could serve as a generally useful alternative to acylated cyanohydrin, which offers diverse structural features in a small space, but is problematic in drug design due to stability issues. Such a concept is similar to using hydroxyisooxazole as nonclassical bioisosteres of a carboxyl group and may find additional applications.<sup>12</sup>

## RESULTS AND DISCUSSION

As previously reported, (**R**)-**1** proved to be one of the most potent EV71 inhibitors currently known (Fig. 1A). Unfortunately, *in vitro* stability studies demonstrated that (**R**)-**1** was rapidly degraded in plasma and liver microsome as shown in Fig. 1B. The half-life ( $t_{1/2}$ ) of (**R**)-**1** in human and mouse plasma was merely 11 min and 7 min, respectively. Its metabolic rate in human and mouse liver microsome was even faster ( $t_{1/2}$  = 8 min and 6 min, respectively).

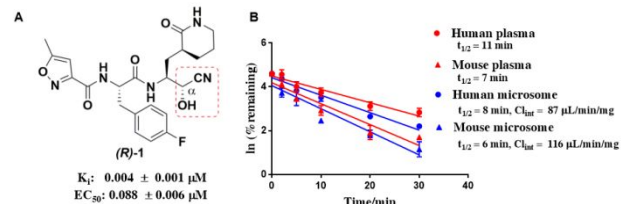
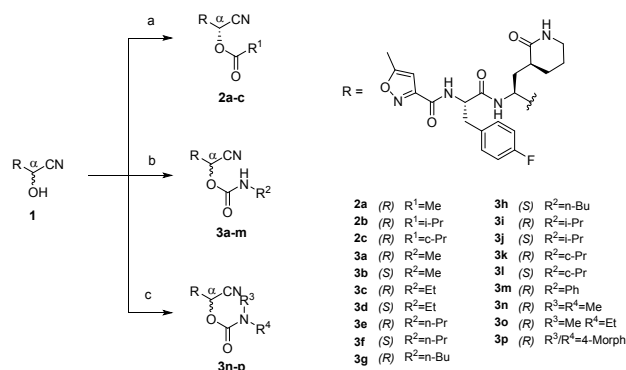


**Figure 1.** A) Structure of (**R**)-**1**; B) The stability of (**R**)-**1** in plasma and microsome. Vertical bars represent the standard deviation of each data point ( $n=3$ ).

Such instability can be attributed to either chemical or metabolic reasons. Physiological pH was shown to enable the reverse reaction of cyanohydrin formation, resulting in the slow release of aldehyde and cyanide (Figure S1), both of which are poisonous and not well-tolerated in drug design.<sup>13</sup> This process was further facilitated in plasma or microsome (Figure S2, S3) probably owing to specific enzymes. In the meantime, a hydroxyl group is susceptible to a series of hepatic metabolic reactions.<sup>14</sup> On the other side, our previous research suggests that the hydroxyl group could tolerate chemical modification to some extent whereas the cyano group should be kept intact to retain the binding affinity.<sup>10</sup> Hence, the hydroxyl group was first derivatized into an ester or a carbamate group in hope of improving chemical or metabolic stability as well as lowering the risk of toxic species (Table 1).

The preparation of (**R**)-**1** was according to the literature.<sup>10</sup> The synthetic route to different derivatives of (**R**)-**1** is outlined in Scheme 1. The esterified derivatives **2a-c** were generally obtained by reacting (**R**)-**1** with acyl chloride under basic conditions. The conditions for preparing carbamate derivatives varied with substitutions on the nitrogen. To synthesize *N*-monosubstituted carbamates **3a-m**, **1** was treated with *N,N'*-carbonyldiimidazole (CDI) to form an active intermediate, which then was reacted with different amines. *N*-Disubstituted carbamates **3n-p** were synthesized by reacting (**R**)-**1** with corresponding carbamoyl chlorides in presence of 4-dimethylaminopyridine (DMAP).

#### Scheme 1. Synthetic Scheme of **2a-c**, **3a-p**<sup>a</sup>



<sup>a</sup> Reagents and conditions: (a) Alkyl chloride, TEA, DCM, 75%; (b) CDI, amine, DCM, 60%; (c) Carbamoyl chloride, DMAP, DCM, 70%.

**Table 1. Enzyme inhibitory activity, antiviral activity and cytotoxicity of **2a-c**, **3a-p** as inhibitors of EV71 3C<sup>pro</sup>**

NO.		$K_i$ ( $\mu\text{M}$ ) <sup>a</sup>	$\text{EC}_{50}$ ( $\mu\text{M}$ ) <sup>a</sup>	$\text{CC}_{50}$ ( $\mu\text{M}$ ) <sup>a</sup>
( <b>R</b> )- <b>1</b>		0.004 ± 0.001	0.088 ± 0.006	>100
<b>2a</b>		0.064 ± 0.005	0.067 ± 0.008	>100
<b>2b</b>		0.24 ± 0.047	2.61 ± 0.12	>100
<b>2c</b>		0.56 ± 0.15	4.93 ± 0.23	>100
<b>3a</b>		0.071 ± 0.017	0.62 ± 0.05	>100
<b>3b</b>		0.046 ± 0.008	1.00 ± 0.09	>100
<b>3c</b>		0.051 ± 0.011	0.75 ± 0.34	>100
<b>3d</b>		0.19 ± 0.037	3.58 ± 0.43	>100
<b>3e</b>		0.085 ± 0.017	0.16 ± 0.06	>100
<b>3f</b>		0.183 ± 0.015	2.21 ± 0.05	>100
<b>3g</b>		0.45 ± 0.007	0.69 ± 0.08	>100
<b>3h</b>		4.78 ± 0.036	8.46 ± 1.52	>100
<b>3i</b>		0.036 ± 0.004	0.65 ± 0.07	>100

1	3j		0.093 ± 0.011	1.73 ± 0.21	>100
2					
3	3k		1.28 ± 0.14	5.11 ± 0.62	>100
4					
5	3l		6.21 ± 0.42	12.83 ± 0.72	>100
6					
7	3m		N.D. <sup>b</sup>	13.18 ± 2.35	>100
8					
9	3n		N.D. <sup>b</sup>	70.40 ± 8.35	>100
10					
11	3o		N.D. <sup>b</sup>	>100	>100
12					
13	3p		N.D. <sup>b</sup>	>100	>100

<sup>a</sup> Each data presents the average results from three independent experiments, and error bars represent SEMs (n=3). <sup>b</sup> Not Detected.

Considering the relatively confined space at the S1' pocket of 3C<sup>Pro</sup> (Figure 3A), esterification was preliminarily limited to several small groups, i.e., methyl, isopropyl and cyclopropyl group. Compared with cyanohydrin (**R**)-**1**, **2a** ( $K_i = 0.064 \pm 0.005 \mu\text{M}$ ,  $\text{EC}_{50} = 0.067 \pm 0.008 \mu\text{M}$ ) showed slightly weaker inhibition against 3C<sup>Pro</sup>. However, both of them exhibited similar antiviral activity, probably because the acetylation of hydroxyl group improved cell permeability of **2a**. Additionally, bulkier groups (**2b** and **2c**) led to reduced inhibition effect, which was in agreement with the narrow S1' pocket. The stability of **2a** in plasma and microsome was examined thereafter (Figure S4). Compared with cyanohydrin (**R**)-**1**, the plasma stability of **2a** was improved by over 5-fold in plasma different sources ( $t_{1/2}$ , human = 50 min and  $t_{1/2}$ , mouse = 42 min). The metabolic half-life of **2a** in human liver microsome was also extended to 64 min, but the improvement of its metabolic stability in mouse liver microsome was negligible. The insufficient stability in mouse microsome has limited study on this class of compounds in the mouse model. Further, the ester group is prone to hydrolysis and could contribute to stability issues *in vivo*.

With the hope of further improving hydrolytic stability, a series of *N*-monosubstituted and *N*-disubstituted carbamate derivatives of **1** were synthesized and tested. From the perspective of steric effect, long-chain alkyl groups (**3h**) or bulky aromatic groups (**3m**) were not easily accommodated by the S1' pocket, similar with the ester derivatives. The impact of  $\alpha$ -carbon stereochemistry on binding was trivial unless the substituent was oversized (e.g., **3g** vs **3h**). In addition, there emerged almost total loss of activity when the carbamate nitrogen was disubstituted (e.g., **3n** vs **3a**). At first glance, the poor activity of **3n** seems aberrant since its structural analogue **2b** ( $K_i = 0.24 \pm 0.047 \mu\text{M}$ ) still possesses fair potency. This is possibly because, compared with **2b**, the planar carbamate scaffold of **3n** restricts the adaptation of two methyl groups thus leading to substantial steric clash with enzyme pocket.

The plasma stability of this class was studied by examining representatives **3e** (best cellular activity), **3i** (best enzyme inhibitory activity), **3o**, and **3p** (*N*-

disubstituted carbamate). As shown in Figure 2A, **3i** ( $t_{1/2, \text{mouse}} = 31 \text{ min}$ ) was more stable than **3e** ( $t_{1/2, \text{mouse}} = 12 \text{ min}$ ) and the same trend was observed in human plasma (Figure S5). Interestingly, *N*-disubstituted carbamate inhibitors **3o** and **3p** showed extremely high plasma stability. Plasma metabolite characterization was performed for **3i** using a tandem MS method to gain a further understanding of the substituent effect. The peak shift in LC indicated **3i** (RT = 6.41 min) was partially converted to another structure (RT = 5.41 min) as shown in Figure 2B. To our surprise, these two structures had an identical *m/z* value of 556 that was assigned to their molecular ions according to the analysis of primary and secondary mass spectra (Figure S7). The same conversion was observed in PBS buffer (pH = 7.4) for **3e** and **3i**, but the conversion of **3e** was remarkably more rapid than **3i**, which coincided with the difference in their plasma half-life. In addition, **3o** and **3p** did not undergo such conversion in PBS buffer (pH = 7.4) (Figure S6). These findings suggest that the conversion of carbamate was plasma-independent and likely an intramolecular reaction involving the carbamate nitrogen. After an extensive literature survey,<sup>15</sup> a prototropic tautomerization mechanism was proposed. Specifically, the nitrogen of *N*-monosubstituted carbamate could nucleophilically attack the well-oriented nitrile under basic condition thus undergoing a cyclization. To validate this assumption, a cyclized carbamate derivative **4e** was chemically synthesized, and it was confirmed by secondary mass spectrometry that the synthesized **4e** and the product auto-converted from **3e** were exactly the same (Figure S8). This mechanism not only explains the identical *m/z* found in original peak and product peak, but also sheds light on the outstanding stability of *N*-disubstituted carbamate derivatives in that at least one hydrogen was required for the proton transfer.

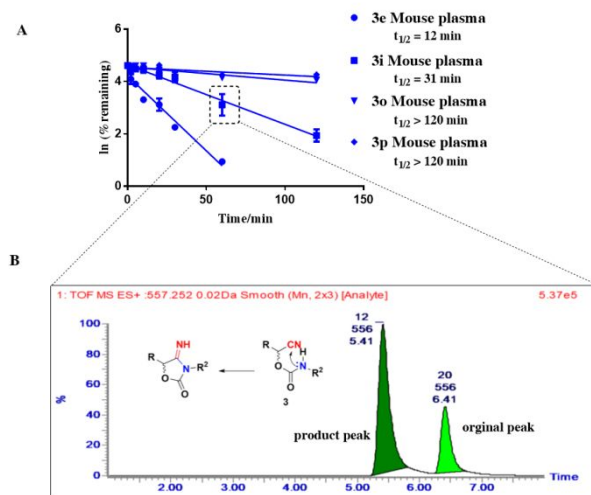
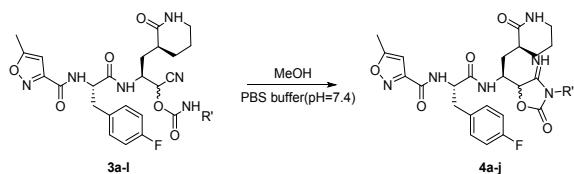


**Figure 2.** A) The stability of represent compounds in mouse plasma. B) LC/MS profile showing the disappearance of **3i** (Retention time = 6.41min) and the appearance of product peak (Retention time = 5.41min) after 60 min of incubation with mouse plasma.

### Scheme 2. Synthetic Scheme of 4a-j



The intriguing auto-conversion of carbamate derivatives encouraged us to study their completely cyclized forms. A series of cyclic carbamate compounds **4** containing the same substituents corresponded to **3** were chemically synthesized and tested (Scheme 2 and Table 2). The SAR of **4** shares a similar trend with that of **3**, i.e. small or branched groups are favored at the S1' pocket. The isopropyl substituted **4g** exhibited the most potent inhibitory activity ( $K_i = 0.033 \pm 0.008 \mu\text{M}$ ,  $\text{EC}_{50} = 0.10 \pm 0.02 \mu\text{M}$ ) among three classes of compounds discussed in this work. A flexible-receptor docking simulation yielded the best binding pose of **4g** that bears some resemblance of a cyanohydrin inhibitor complexed with 3C<sup>pro</sup> (Figure 3A). In particular, the atoms of imine and bridging oxygen in 4-iminooxazolidin-2-one moiety has a very similar spatial arrangement with corresponding atoms in cyanohydrin moiety. The carbonyl oxygen of 4-iminooxazolidin-2-one moiety forms a strong hydrogen bond (2.2 Å) with His40, which is also an important interaction found in the crystal structure. Based on these features, 4-iminooxazolidin-2-one can be regarded as a nonclassical bioisostere of the cyanohydrin structure. Furthermore, the side chains of Phe25 and Ala144 provide the isopropyl group with a favorable hydrophobic environment (Fig. 3B). Compared with **3**, a noteworthy detail was that the superiority of (*R*)-**4** over (*S*)-**4** became more obvious. For example, **4c** ( $K_i = 0.22 \pm 0.05 \mu\text{M}$ ) and **4e** ( $K_i = 0.083 \pm 0.01 \mu\text{M}$ ) were substantially more potent than their counterparts **4d** ( $K_i = 3.53 \pm 0.24 \mu\text{M}$ ) and **4f** ( $K_i = 2.60 \pm 0.81 \mu\text{M}$ ). In contrast, the differences between diastereomers of the corresponding uncyclized carbamate compounds (**3c** vs **3d** and **3e** vs **3f**) were relatively minor. Apparently, the noncyclic structure of **3** allowed for adequate adjustment of substituents during induced-fit process, whereas the inflexibility of cyclized structure of **4** likely prevents such adjustment. On account of the fact that preceding SAR discussion was premised on noncovalent interaction, this issue was investigated by incubating 3C<sup>pro</sup> with (*R*)-**1** or **4e** prior to trypsin digestion (Figure S11, S12). The LC-MS/MS results of digested peptide fragments indicated that neither was bonded to the catalytic cysteine compared to AG7088 (a covalent inhibitor of EV71 3C<sup>pro</sup>), ruling out the possibility of covalent inhibitors.<sup>16</sup>

**Table 2. Enzyme inhibitory activity, antiviral activity and cytotoxicity of 4a-j as EV71 3C<sup>pro</sup> inhibitors**

NO.	$K_i$ ( $\mu\text{M}$ ) <sup>a</sup>	$\text{EC}_{50}$ ( $\mu\text{M}$ ) <sup>a</sup>	$\text{CC}_{50}$ ( $\mu\text{M}$ ) <sup>a</sup>
<b>4a</b>	$0.28 \pm 0.07$	$3.97 \pm 0.50$	>100

<b>4b</b>	$0.21 \pm 0.04$	$1.03 \pm 0.21$	>100
<b>4c</b>	$0.22 \pm 0.05$	$4.37 \pm 0.60$	>100
<b>4d</b>	$3.53 \pm 0.24$	$17.16 \pm 0.80$	>100
<b>4e</b>	$0.083 \pm 0.01$	$0.21 \pm 0.05$	>100
<b>4f</b>	$2.60 \pm 0.81$	$12.67 \pm 1.71$	>100
<b>4g</b>	$0.033 \pm 0.008$	$0.10 \pm 0.02$	>100
<b>4h</b>	$0.061 \pm 0.06$	$0.51 \pm 0.08$	>100
<b>4i</b>	$1.71 \pm 0.11$	$8.81 \pm 1.42$	>100
<b>4j</b>	$2.54 \pm 0.32$	$12.73 \pm 2.83$	>100

<sup>a</sup> Each data presents the average results from three independent experiments, and error bars represent SEMs (n=3).

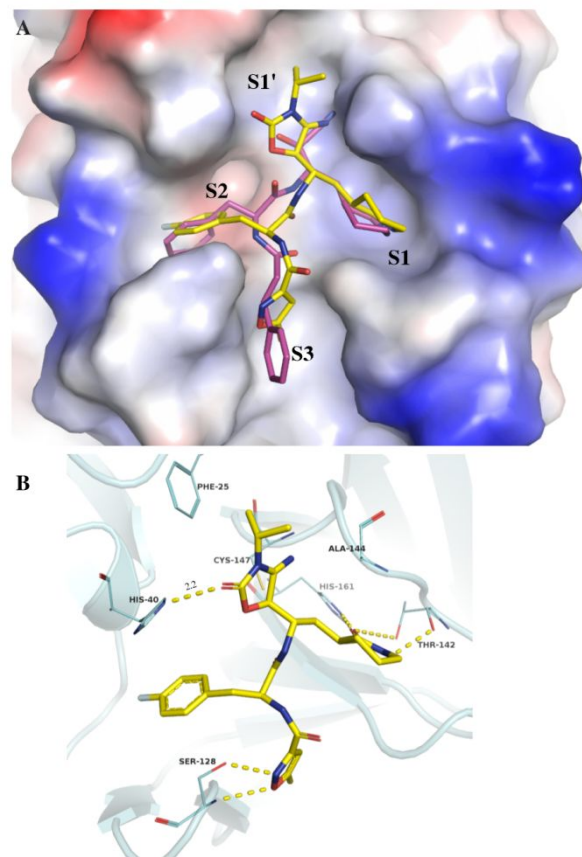


**Figure 3. Docking result.** A) The docked **4g** (yellow) were superimposed with a co-crystal structure of a cyanohydrin

inhibitor (magenta) complexed with 3C<sup>pro</sup> (PDB code: 5BPE); B) Key interactions between **4g** and surrounding residues.

No spontaneous ring-opening was observed for **4e** and **4g** in human and mouse plasma within at least 2 hours (the duration of the study, Figure 4A). The excellent stability of both **4** and *N*-disubstituted **3** implies that a tertiary amine structure could drastically prevent the hydrolysis in plasma. In liver microsomal stability assays, both compounds showed substantially improved metabolic stability compared with (*R*)-**1**. The clearance in microsomal incubation ( $Cl_{int}$ ) of **4e** and **4g** was determined to be 9-20  $\mu\text{L}/\text{min}/\text{mg}$  (Figure 4B). As an estimation of the risk of *in vivo* first pass metabolism, the data suggested these compounds were subject to low risk of first pass metabolism according to a general classification of  $Cl_{int}$ .<sup>17</sup> Moreover, unlike **2a**, the data consistency across species of **4e** and **4g** manifested the robustness of this class of compounds.

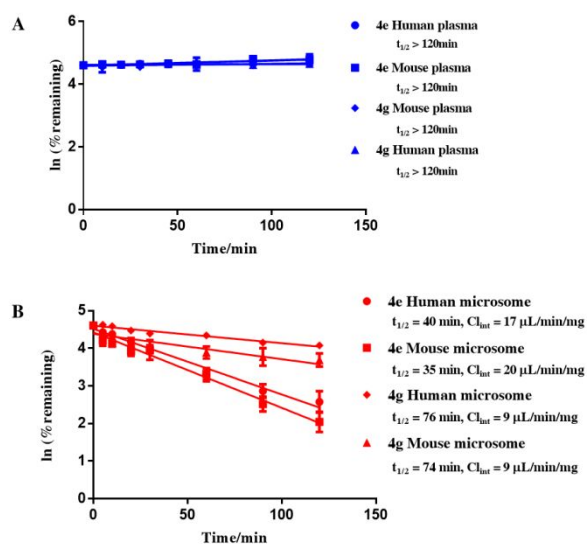


**Figure 4.** A) The stability of **4e**, **4g** in human and mouse plasma; B) The stability of **4e**, **4g** in human and mouse microsomes (1.0 mg/mL). Vertical bars represent the standard deviation of each data point ( $n=3$ ).

In view of the potent activity as well as improved microsomal and plasma stability of 4-iminoxazolidin-2-one inhibitors, **4e** was first selected for *in vivo* pharmacokinetic studies in mice. **4e** was administered orally (PO) and intravenous (IV) to groups of male mice with a single dose of 20 mg/kg (Figure 5). The results showed that, after IV administration of 20.00 mg/kg **4e**, the peak plasma concentration ( $C_{max}$ ) in mice was 8.2 mg/mL at 5 min. Presenting high drug exposure level ( $AUC_{0-t} = 140.1 \text{ mg}\cdot\text{mL}^{-1}\cdot\text{min}$ ), and the terminal elimination half-life ( $t_{1/2}$ ) was 51 min. Moreover, the compound was quickly absorbed after oral dosing at 20 mg/kg **4e** and reached a peak plasma concentration of 0.15 mg/mL at 15 min. At the same time, **4e** possessed a moderate half-life of 60 min and a reasonable plasma exposure of  $7.9 \text{ mg}\cdot\text{mL}^{-1}\cdot\text{min}$ , yet its absolute bioavailability was relatively low and that needs to be improved in the followed studies.

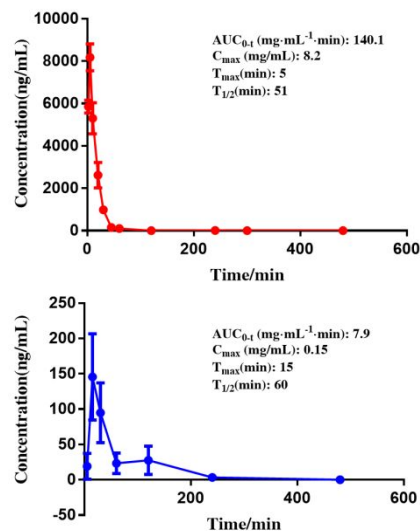


**Figure 5.** A) Plasma concentration time profile following Intravenous Administration of 20mg/kg **4e**; B) Plasma concentration time profile following Oral Administration of 20 mg/kg **4e**. Each point represents mean  $\pm$  SD ( $n=3$ ).

## CONCLUSION

An important class of EV71 3C<sup>pro</sup> inhibitors such as (*R*)-**1** is very promising for further development, but suffer from inherent stability and potential toxicity problems because of the use of a cyanohydrin warhead. The known stability and toxicity of cyanohydrins, which releases cyanide upon hydrolysis, led to the work to either stabilize this group or find a replacement. In doing so, we first took advantage of the hydroxyl group in (*R*)-**1** for further derivatization for improved stability. In the course of modification, we find nonclassical bioisosteric replacements of cyanohydrin moiety with 4-iminoxazolidin-2-one, which resulted in identification of novel compound series **4**. Among them, **4e** and **4g** showed the most potent inhibitory activity with greatly improved stability. Preliminary *in vivo* pharmacokinetic studies of **4e** also manifested moderate PK properties. Overall, 4-iminoxazolidin-2-one moiety does appear to serve as a nonclassical bioisostere to the labile cyanohydrin moiety for circumventing potential disadvantages. Further, the successful replacement of acyl cyanohydrin with 4-iminoxazolidin-2-one also opens doors to its further development as a generally applicable bioisostere of the cyanohydrin moiety.

## EXPERIMENTAL SECTION

**General.** All reagents were purchased from commercial suppliers and used as received. NMR spectra were recorded on a Bruker AVANCE-400 (400 MHz for <sup>1</sup>H and 101 MHz for <sup>13</sup>C) (Bruker, Karlsruhe, Germany) NMR spectrometer. Molecular mass was determined by ESI mass spectrometry using a Shimadzu LCMS-2020 (Shimadzu, Kyoto, Japan). Optical rotations were measured with an Insmark IP-120 Automatic Polarimeter (Insmark, Shanghai, China). Measurements were collected at 20 °C in MeOH at 589 nm.  $[\alpha]_D$  values are given in units of ( $^{\circ} \times \text{mL}$ )/(g  $\times$  dm). HRMS were recorded on a high-resolution ESI-FTICR mass spectrometer (Varian 7.0 T, Varian, USA). All tested compounds exhibited purities of  $> 95\%$  as analyzed by HPLC (Dionex UltiMate 3000, Germany).

### General Procedure for the Synthesis of ester derivatives **2a-c**.

**Preparation of **2a**.** A solution of (*R*)-**1** (200 mg, 0.42 mmol) in anhydrous  $\text{CH}_2\text{Cl}_2$  (50 mL), acetyl chloride (0.06 mL, 0.84 mmol) and TEA (0.18 mL, 1.27 mmol) were added dropwise at 0 °C. Then the

reaction mixture was stirred at room temperature for 2 h, followed by washing with H<sub>2</sub>O (100 mL×2), saturated citric acid solution (100 mL×2), saturated NaHCO<sub>3</sub> solution (100 mL×2) and brine (100 mL×2). The organic phase was dried over Na<sub>2</sub>SO<sub>4</sub> and concentrated, and the residue was purified by silica gel column chromatography (MeOH: DCM = 1: 70 v/v) to afford the pure product as a white solid **2a** (174 mg, 80%). [ $\alpha$ ]<sub>D</sub><sup>20</sup> = -43.95 (c = 0.012, MeOH). <sup>1</sup>H NMR (CDCl<sub>3</sub>-d)  $\delta$  8.33 (d, *J* = 7.2 Hz, 1H), 7.57 (d, *J* = 8.3 Hz, 1H), 7.24 – 7.14 (m, 2H), 7.02 – 6.90 (m, 2H), 6.79 (s, 1H), 6.32 (d, *J* = 1.0 Hz, 1H), 5.32 (d, *J* = 5.0 Hz, 1H), 4.93 (q, *J* = 7.2 Hz, 1H), 4.23 (s, 1H), 3.28 (p, *J* = 5.7, 4.5 Hz, 2H), 3.11 (qd, *J* = 13.9, 6.7 Hz, 2H), 2.43 (s, 3H), 2.33 (s, 1H), 2.22 (ddt, *J* = 13.7, 10.8, 4.5 Hz, 1H), 2.12 (s, 3H), 2.00 (d, *J* = 8.7 Hz, 1H), 1.85 (dt, *J* = 12.9, 4.8 Hz, 1H), 1.71 (ddd, *J* = 13.8, 7.7, 3.2 Hz, 2H), 1.49 (dtd, *J* = 13.5, 10.9, 3.1 Hz, 1H). <sup>13</sup>C NMR (CDCl<sub>3</sub>-d)  $\delta$  175.0, 171.5, 171.2, 168.7, 162.0 (d, *J* = 245.3 Hz), 158.9, 158.2, 131.8 (d, *J* = 3.1 Hz), 130.9, 130.9, 115.7, 115.4, 115.1, 101.4, 62.7, 54.4, 48.5, 42.2, 37.8, 37.5, 31.0, 27.0, 21.3, 20.3, 12.3. HRMS (ESMS): C<sub>25</sub>H<sub>28</sub>FN<sub>5</sub>NaO<sub>6</sub> (M + Na)<sup>+</sup>, calcd. 536.1916, found 536.1920.

#### General Procedure for the Synthesis of carbamate derivatives **3a-p**.

**Preparation of 3a.** To a solution of (**R**)-**1** (200 mg, 0.42 mmol) in anhydrous CH<sub>2</sub>Cl<sub>2</sub> (50 mL), *N,N'*-carbonyldiimidazole (103.2 mg, 0.64 mmol) in dry CH<sub>2</sub>Cl<sub>2</sub> was added dropwise over a period of 30 min under nitrogen atmosphere at 0 °C. After stirring at room temperature for 30 min, methylamine (2M solution in THF) (0.64 mL, 1.27 mmol) was added and the reaction mixture was stirred at room temperature for 2 h, followed by washing with H<sub>2</sub>O (100 mL×2), saturated citric acid solution (100 mL×2), saturated NaHCO<sub>3</sub> solution (100 mL×2) and brine (100 mL×2). The organic phase was dried over Na<sub>2</sub>SO<sub>4</sub> and concentrated, and the residue was purified by column chromatography (MeOH: DCM = 1: 60 v/v) to afford the pure product as a white solid **3a** (143 mg, 64%). [ $\alpha$ ]<sub>D</sub><sup>20</sup> = -48.71 (c = 0.058, MeOH). <sup>1</sup>H NMR (CDCl<sub>3</sub>-d)  $\delta$  8.13 (d, *J* = 8.0 Hz, 1H), 7.64 (d, *J* = 8.6 Hz, 1H), 7.24 – 7.11 (m, 2H), 6.94 (t, *J* = 8.6 Hz, 2H), 6.62 (s, 1H), 6.30 (s, 1H), 5.33 – 5.26 (m, 1H), 5.23 (q, *J* = 4.7 Hz, 1H), 5.03 (q, *J* = 7.4 Hz, 1H), 4.34 (dp, *J* = 12.8, 3.7 Hz, 1H), 3.25 (d, *J* = 6.9 Hz, 2H), 3.16 (dd, *J* = 13.9, 6.3 Hz, 1H), 3.06 (dd, *J* = 13.8, 7.4 Hz, 1H), 2.80 (s, 3H), 2.42 (s, 3H), 2.35 (td, *J* = 13.0, 3.9 Hz, 1H), 2.22 (tt, *J* = 10.0, 6.5 Hz, 1H), 2.07 – 1.93 (m, 1H), 1.90 – 1.76 (m, 1H), 1.71 – 1.57 (m, 2H), 1.44 (s, 1H). <sup>13</sup>C NMR (CDCl<sub>3</sub>-d)  $\delta$  174.5, 171.4, 171.2, 161.9 (d, *J* = 245.1 Hz), 158.9, 158.2, 154.4, 132.0 (d, *J* = 3.1 Hz), 131.0, 130.9, 115.9, 115.5, 115.3, 101.3, 64.0, 54.3, 48.2, 42.2, 38.1, 37.4, 31.3, 27.7, 26.6, 21.4, 12.3. HRMS (ESMS): C<sub>25</sub>H<sub>29</sub>FN<sub>6</sub>NaO<sub>6</sub> (M + Na)<sup>+</sup>, calcd. 551.2025, found 551.2029.

**Preparation of 3n.** To a solution of (**R**)-**1** (200 mg, 0.42 mmol) in anhydrous CH<sub>2</sub>Cl<sub>2</sub> (50 mL), dimethylcarbamoyl chloride (0.08 mL, 0.85 mmol) in dry CH<sub>2</sub>Cl<sub>2</sub> was added dropwise at 0 °C, followed by addition of DMAP (0.21 mg, 1.7 mmol). Then the reaction mixture was stirred at room temperature for 4 h, followed by washing with H<sub>2</sub>O (100 mL×2), saturated citric acid solution (100 mL×2), saturated NaHCO<sub>3</sub> solution (100 mL×2) and brine (100 mL×2). The organic phase was dried over Na<sub>2</sub>SO<sub>4</sub> and concentrated, and the residue was purified by column chromatography (MeOH: DCM = 1: 60 v/v) to afford the pure product as a white solid **3n** (140 mg, 61%). [ $\alpha$ ]<sub>D</sub><sup>20</sup> = -45.29 (c = 0.057, MeOH). <sup>1</sup>H NMR (CDCl<sub>3</sub>-d)  $\delta$  8.20 (d, *J* = 8.0 Hz, 1H), 7.62 (d, *J* = 8.5 Hz, 1H), 7.17 (dd, *J* = 8.2, 5.3 Hz, 2H), 6.93 (t, *J* = 8.5 Hz, 2H), 6.57 (s, 1H), 6.29 (s, 1H), 5.38 – 5.22 (m, 1H), 4.97 (q, *J* = 7.4 Hz, 1H), 4.35 (tt, *J* = 11.7, 5.1 Hz, 1H), 3.31 – 3.20 (m, 2H), 3.15 (dd, *J* = 13.9, 6.1 Hz, 1H), 3.04 (dd, *J* = 13.9, 7.6 Hz, 1H), 2.89 (d, *J* = 15.7 Hz, 6H), 2.41 (s, 3H), 2.35 (dd, *J* = 13.6, 3.9 Hz, 1H), 2.28 – 2.13 (m, 1H), 2.00 (h, *J* = 5.0 Hz, 1H), 1.82 (dt, *J* = 14.5, 4.4 Hz, 1H), 1.75 – 1.58 (m, 2H), 1.56 – 1.39 (m, 1H). <sup>13</sup>C NMR (CDCl<sub>3</sub>-d)  $\delta$  174.4, 171.4, 171.1, 161.9 (d, *J* = 245.1 Hz), 158.8, 158.2, 153.7, 132.0 (d, *J* = 3.1 Hz), 130.9, 130.8, 116.0, 115.5, 115.3, 101.4, 64.4, 54.4, 48.5, 42.2, 37.9, 37.5, 36.8, 36.0, 31.4, 26.7, 21.3, 12.2. HRMS (ESMS): C<sub>26</sub>H<sub>31</sub>FN<sub>6</sub>NaO<sub>6</sub> (M + Na)<sup>+</sup>, calcd. 565.2181, found 565.2184.

#### General Procedure for the Synthesis cyclic carbamate (4-iminooxazolidin-2-one) derivatives of **4a-h**.

**Preparation of 4a.** A solution of compound **3a** (200.0 mg, 0.38 mmol) in MeOH: PBS buffer (pH = 7.4) = 1:2 v/v, the reaction mixture was stirred at room temperature for 4 h. The solvent was removed under vacuum. The aqueous layer was extracted with DCM (100 mL×3). The combined organic layer was dried over anhydrous sodium sulfate and concentrated, and the residue was purified by ether recrystallization

to afford the pure product as a white solid **4a** (128 mg, 64%). [ $\alpha$ ]<sub>D</sub><sup>20</sup> = -15.83 (c = 0.063, MeOH). <sup>1</sup>H NMR (CDCl<sub>3</sub>-d)  $\delta$  8.49 (d, *J* = 8.2 Hz, 1H), 7.70 (d, *J* = 8.7 Hz, 1H), 7.60 (s, 1H), 7.14 (dd, *J* = 8.4, 5.3 Hz, 2H), 6.91 (t, *J* = 8.3 Hz, 2H), 6.58 (s, 1H), 6.31 (s, 1H), 4.95 (d, *J* = 2.7 Hz, 1H), 4.88 (dt, *J* = 8.5, 4.4 Hz, 1H), 4.55 (s, 1H), 3.27 (dd, *J* = 9.5, 4.7 Hz, 2H), 3.14 – 3.01 (m, 2H), 2.94 (s, 3H), 2.42 (d, *J* = 3.4 Hz, 4H), 2.17 – 2.11 (m, 1H), 2.03 (ddt, *J* = 12.6, 5.9, 2.9 Hz, 1H), 1.89 – 1.80 (m, 1H), 1.67 (q, *J* = 11.2, 9.9 Hz, 1H), 1.58 (ddd, *J* = 14.2, 8.4, 3.1 Hz, 1H), 1.50 (dd, *J* = 12.1, 9.1 Hz, 1H). <sup>13</sup>C NMR (CDCl<sub>3</sub>-d)  $\delta$  174.8, 171.7, 171.2, 161.9 (d, *J* = 245.3 Hz), 161.5, 159.0, 158.2, 156.1, 131.9 (d, *J* = 3.1 Hz), 130.8, 130.7, 115.6, 115.3, 101.6, 79.5, 54.7, 47.7, 42.3, 37.8, 37.5, 31.6, 26.8, 26.3, 21.2, 12.3. HRMS (ESMS): C<sub>25</sub>H<sub>29</sub>FN<sub>6</sub>NaO<sub>6</sub> (M + Na)<sup>+</sup>, calcd. 551.2025, found 551.2030.

## ASSOCIATED CONTENT

### Supporting Information.

Detailed synthetic procedures, the stability study of (**R**)-**1**, the stability study of **2a** and **3**, mass spectra of original and product peak of **3i**, mass spectra of **3e** and **4e**, bioassays, plasma and microsome assay, pharmacokinetic studies, MS spectrum of modified peptide from trypsin digestion, and <sup>1</sup>H NMR, <sup>13</sup>C NMR data for tested compounds (PDF).

Molecular formula strings and some data (CSV).

This material is available free of charge via the Internet at <http://pubs.acs.org>.

## AUTHOR INFORMATION

### Corresponding Author

\* For L.S.: shanglq@nankai.edu.cn; for B.W.: wang@gsu.edu.

### Notes

The authors declare no competing financial interests.

## ACKNOWLEDGMENTS

This work was supported by the National Key Research and Development Program of China (Grant No. 2018YFA0507204), the National Natural Science Foundation of China (Grant No. 21672115) and the State Key Laboratory of Medicinal Chemical Biology.

## ABBREVIATIONS USED

EV71, enterovirus 71; 3C<sup>pro</sup>, 3C protease; SARS CoV M<sup>pro</sup>, severe acute respiratory syndrome coronaviruses main protease; Cl<sub>int</sub>, intrinsic clearance; CDI, *N*, *N'*-carbonyldiimidazole; AUC<sub>0-t</sub>, area under the curve between 0-t.

## REFERENCES

- (1) Zhu, Y.; Jiang, Z.; Xiao, G.; Cheng, S.; Wen, Y.; Wan, C. Circadian rhythm disruption was observed in hand, foot, and mouth disease patients. *Medicine (Baltimore)* **2015**, *94*, e601.
- (2) (a) Shang, L.; Xu, M.; Yin, Z. Antiviral drug discovery for the treatment of enterovirus 71 infections. *Antiviral Res.* **2013**, *97*, 183-194; (b) Chang, L. Y.; Huang, L. M.; Gau, S. S.; Wu, Y. Y.; Hsia, S. H.; Fan, T. Y.; Lin, K. L.; Huang, Y. C.; Lu, C. Y.; Lin, T. Y. Neurodevelopment and cognition in children after enterovirus 71 infection. *N. Engl. J. Med.* **2007**, *356*, 1226-1234.
- (3) (a) Liu, L.; Zhang, Y.; Wang, J.; Zhao, H.; Jiang, L.; Che, Y.; Shi, H.; Li, R.; Mo, Z.; Huang, T.; Liang, Z.; Mao, Q.; Wang, L.; Dong, C.; Liao, Y.; Guo, L.; Yang, E.; Pu, J.; Yue, L.; Zhou, Z.; Li, Q. Study of the integrated immune response induced by an inactivated EV71 vaccine. *PLoS One* **2013**, *8*, e54451; (b) Li, J. X.; Mao, Q. Y.; Liang, Z. L.; Ji, H.; Zhu, F. C. Development of enterovirus 71 vaccines: from

the lab bench to Phase III clinical trials. *Expert. Rev. Vaccines* **2014**, *13*, 609-618.

(4) Brown, B. A., Pallansch, M.A. Complete nucleotide sequence of enterovirus 71 is distinct from poliovirus. *Virus Res.* **1995**, 195-205.

(5) Li, M. L.; Hsu, T. A.; Chen, T. C.; Chang, S. C.; Lee, J. C.; Chen, C. C.; Stollar, V.; Shih, S. R. The 3C protease activity of enterovirus 71 induces human neural cell apoptosis. *Virology* **2002**, *293*, 386-395.

(6) (a) Dragovich, P. S.; Prins, T. J.; Zhou, R.; Fuhrman, S. A.; Patick, A. K.; Matthews, D. A.; Ford, C. E.; Meador, J. W., 3rd; Ferre, R. A.; Worland, S. T. Structure-based design, synthesis, and biological evaluation of irreversible human rhinovirus 3C protease inhibitors. 3. Structure-activity studies of ketomethylene-containing peptidomimetics. *J. Med. Chem.* **1999**, *42*, 1203-1212; (b) Dragovich, P. S.; Webber, S. E.; Babine, R. E.; Fuhrman, S. A.; Patick, A. K.; Matthews, D. A.; Reich, S. H.; Marakovits, J. T.; Prins, T. J.; Zhou, R.; Tikhe, J.; Littlefield, E. S.; Bleckman, T. M.; Wallace, M. B.; Little, T. L.; Ford, C. E.; Meador, J. W., 3rd; Ferre, R. A.; Brown, E. L.; Binford, S. L.; DeLisle, D. M.; Worland, S. T. Structure-based design, synthesis, and biological evaluation of irreversible human rhinovirus 3C protease inhibitors. 2. Peptide structure-activity studies. *J. Med. Chem.* **1998**, *41*, 2819-2834; (c) Dragovich, P. S.; Prins, T. J.; Zhou, R.; Fuhrman, S. A.; Patick, A. K.; Matthews, D. A.; Ford, C. E.; Meador, J. W., 3rd; Ferre, R. A.; Worland, S. T. Structure-based design, synthesis, and biological evaluation of irreversible human rhinovirus 3C protease inhibitors. 1. Structure-activity studies of ketomethylene-containing peptidomimetics. *J. Med. Chem.* **1999**, *42*, 1203-1212.

(7) Kuo, C. J.; Shie, J. J.; Fang, J. M.; Yen, G. R.; Hsu, J. T.; Liu, H. G.; Tseng, S. N.; Chang, S. C.; Lee, C. Y.; Shih, S. R.; Liang, P. H. Design, synthesis, and evaluation of 3C protease inhibitors as anti-enterovirus 71 agents. *Bioorg. Med. Chem.* **2008**, *16*, 7388-7398.

(8) (a) Wu, C.; Cai, Q.; Chen, C.; Li, N.; Peng, X.; Cai, Y.; Yin, K.; Chen, X.; Wang, X.; Zhang, R.; Liu, L.; Chen, S.; Li, J.; Lin, T. Structures of enterovirus 71 3C proteinase (strain E2004104-TW-CDC) and its complex with rupintrivir. *Acta Crystallogr. D Biol. Crystallogr.* **2013**, *69*, 866-871; (b) Wang, J.; Fan, T.; Yao, X.; Wu, Z.; Guo, L.; Lei, X.; Wang, J.; Wang, M.; Jin, Q.; Cui, S. Crystal structures of enterovirus 71 3C protease complexed with rupintrivir reveal the roles of catalytically important residues. *J. Virol.* **2011**, *85*, 10021-10030.

(9) (a) Zhai, Y.; Ma, Y.; Ma, F.; Nie, Q.; Ren, X.; Wang, Y.; Shang, L.; Yin, Z. Structure-activity relationship study of peptidomimetic aldehydes as enterovirus 71 3C protease inhibitors. *Eur. J. Med. Chem.* **2016**, *124*, 559-573; (b) Zeng, D.; Ma, Y.; Zhang, R.; Nie, Q.; Cui, Z.; Wang, Y.; Shang, L.; Yin, Z. Synthesis and structure-activity relationship of alpha-keto amides as enterovirus 71 3C protease inhibitors. *Bioorg. Med. Chem. Lett.* **2016**, *26*, 1762-1766.

(10) Zhai, Y.; Zhao, X.; Cui, Z.; Wang, M.; Wang, Y.; Li, L.; Sun, Q.; Yang, X.; Zeng, D.; Liu, Y.; Sun, Y.; Lou, Z.; Shang, L.; Yin, Z. Cyanohydrin as an anchoring group for potent and selective inhibitors of enterovirus 71 3C protease. *J. Med. Chem.* **2015**, *58*, 9414-9420.

(11) Fomunyan, R. T.; Adegbola, A. A.; Oke, O. L. The stability of cyanohydrins. *Food Chem.* **1985**, *17*, 221-225.

(12) (a) Krehan, D.; Frølund, B.; Ebert, B.; Nielsen, B.; Krogsgaard-Larsen, P.; Johnston, G. A. R.; Chebib, M. Aza-THIP and related analogues of THIP as GABA C antagonists. *Biorg. Med. Chem.* **2003**, *11*, 4891-4896; (b) Lima, L. M.; Barreiro, E. J. Bioisosterism: a useful strategy for molecular modification and drug design. *Curr. Med. Chem.* **2005**, *12*, 23-49.

(13) De Nicola, G. R.; Leoni, O.; Malaguti, L.; Bernardi, R.; Lazzeri, L. A simple analytical method for dhurrin content evaluation in cyanogenic plants for their utilization in fodder and biofumigation. *J. Agric. Food Chem.* **2011**, *59*, 8065-8069.

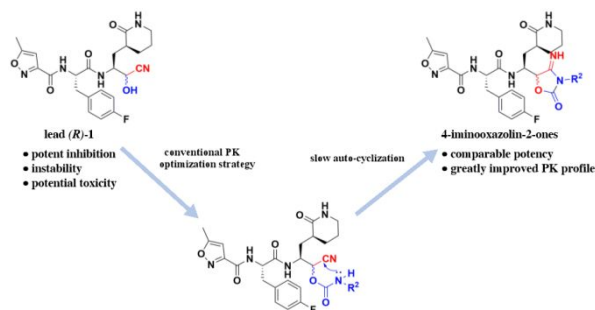
(14) Kerns, E. H.; Di, L., Chapter 11 - Metabolic Stability. In *Drug-like Properties: Concepts, Structure Design and Methods*, Kerns, E. H.; Di, L., Eds. Academic Press: San Diego, 2008; pp 137-II.

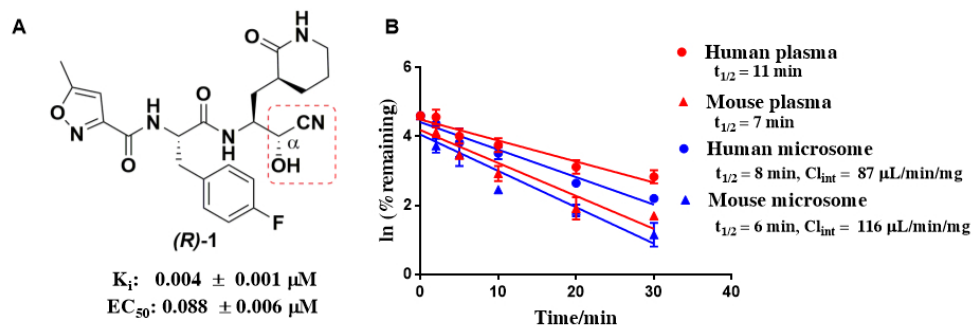
(15) (a) Kurz, T.; Widyan, K. O-Protected 3-hydroxy-oxazolidin-2,4-diones: novel precursors in the synthesis of alpha-hydroxyhydroxamic acids. *Org. Biomol. Chem.* **2004**, *2*, 2023-2027; (b) Kurz, T.; Widyan, K. Microwave-assisted conversion of N-substituted oxazolidin-2,4-diones into  $\alpha$ -hydroxyamides. *Tetrahedron* **2005**, *61*, 7247-7251.

(16) Lu, G.; Qi, J.; Chen, Z.; Xu, X.; Gao, F.; Lin, D.; Qian, W.; Liu, H.; Jiang, H.; Yan, J.; Gao, G. F. Enterovirus 71 and coxsackievirus A16 3C proteases: binding to rupintrivir and their substrates and anti-hand, foot, and mouth disease virus drug design. *J. Virol.* **2011**, *85*, 10319-10331.

(17) Gising, J.; Belfrage, A. K.; Alogheli, H.; Ehrenberg, A.; Akerblom, E.; Svensson, R.; Artursson, P.; Karlen, A.; Danielson, U. H.; Larhed, M.; Sandstrom, A. Achiral pyrazinone-based inhibitors of the hepatitis C virus NS3 protease and drug-resistant variants with elongated substituents directed toward the S2 pocket. *J. Med. Chem.* **2014**, *57*, 1790-1801.

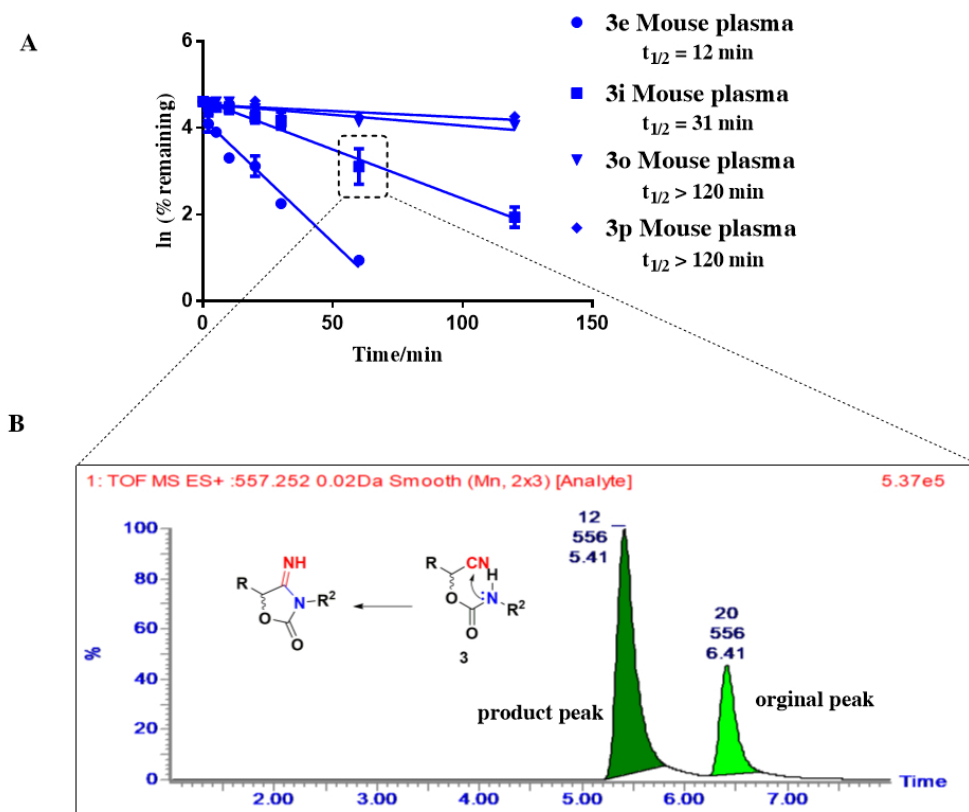
## TOC





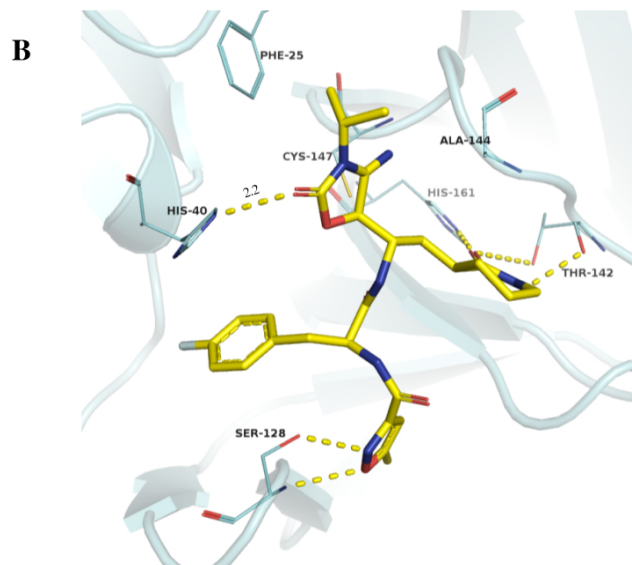
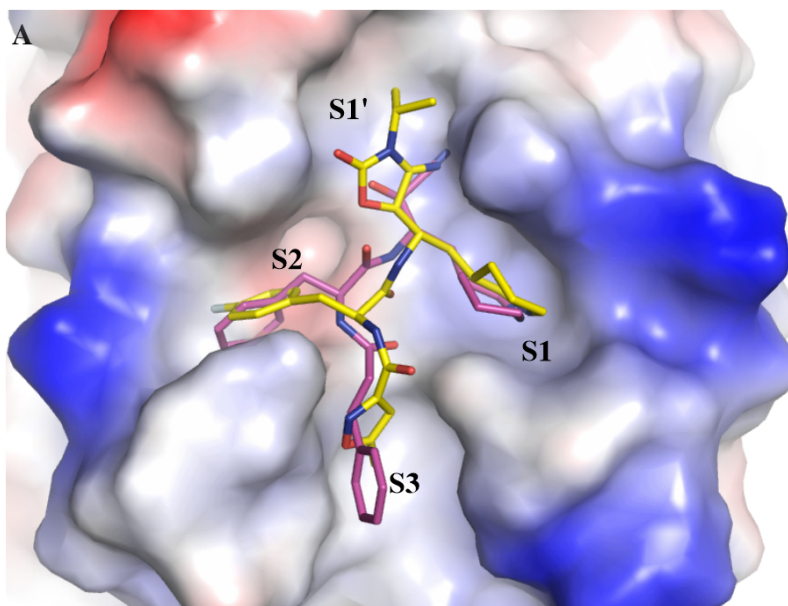
A) Structure of **(R)-1**; B) The stability of **(R)-1** in plasma and microsomes. Vertical bars represent the standard deviation of each data point ( $n=3$ ).

80x29mm (300 x 300 DPI)



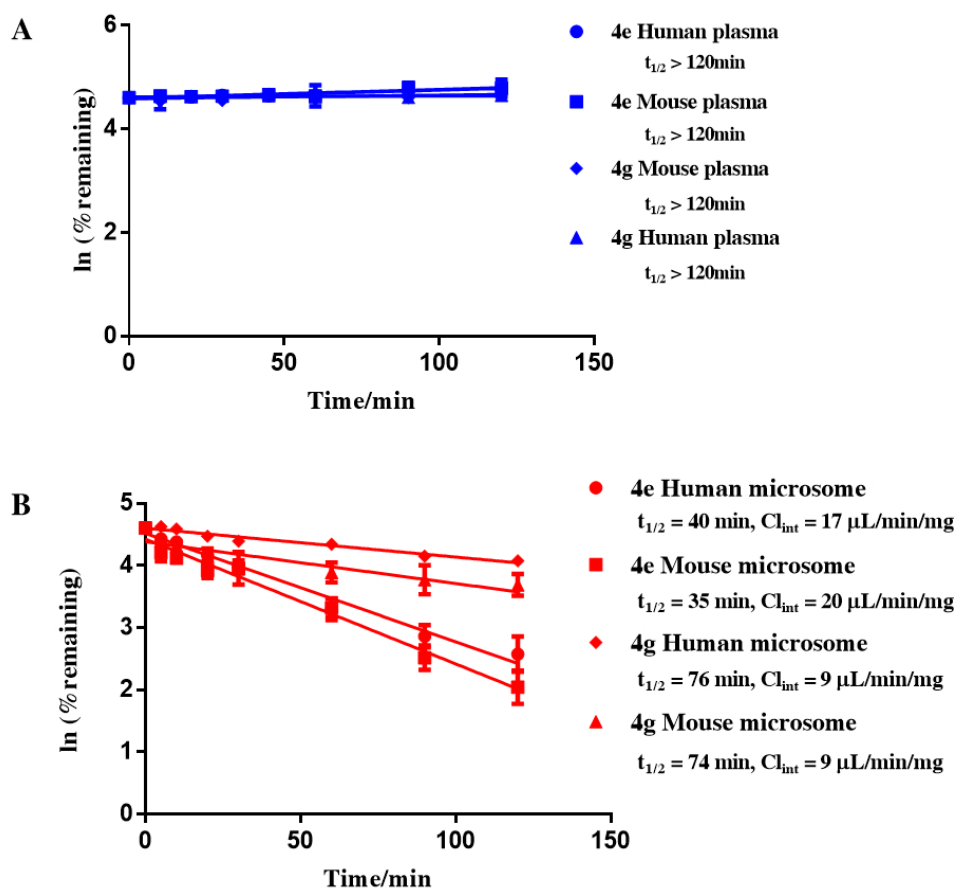
34 A) The stability of represent compounds in mouse plasma. B) LC/MS profile showing the disappearance of **3i**  
35 (Retention time = 6.41min) and the appearance of product peak (Retention time = 5.41min) after 60 min of  
36 incubation with mouse plasma.

37 80x68mm (300 x 300 DPI)



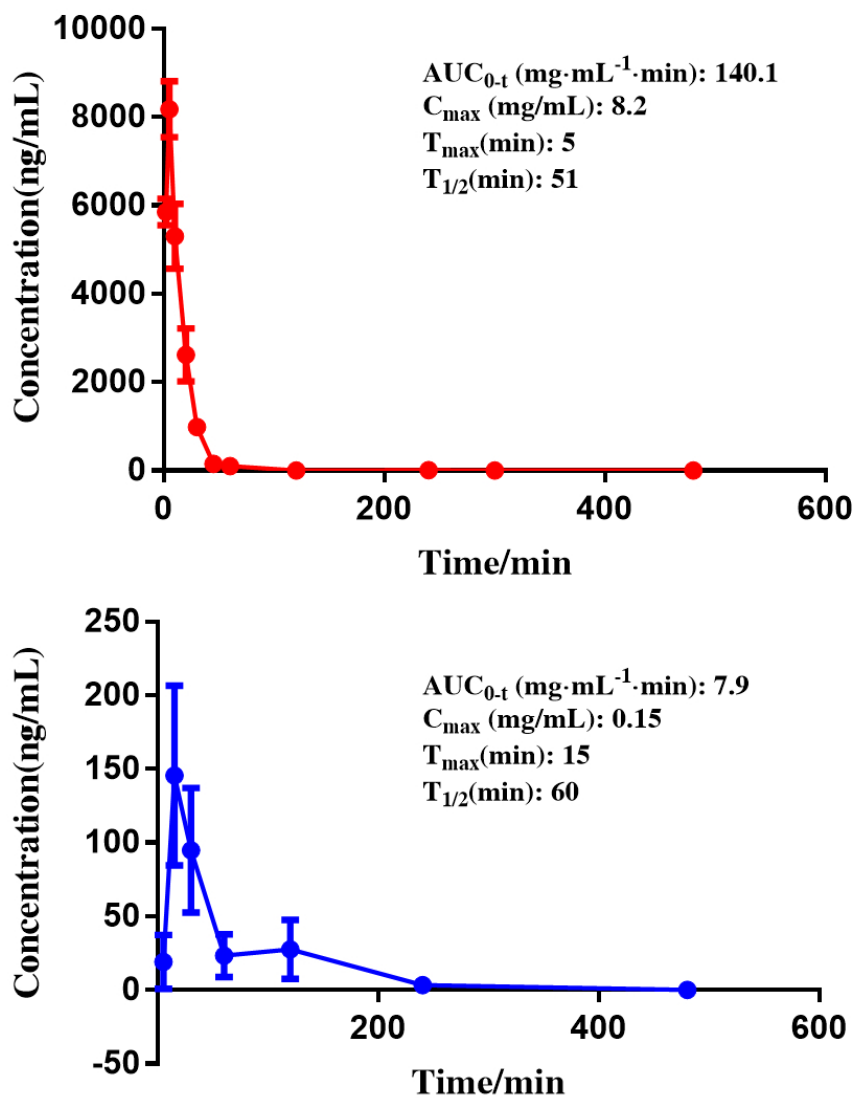
45 Docking result. A) The docked **4g** (yellow) were superimposed with a co-crystal structure of a cyanohydrin  
46 inhibitor (magenta) complexed with 3C<sup>Pf0</sup> (PDB code: 5BPE); B) Key interactions between **4g** and  
47 surrounding residues.

48 80x115mm (300 x 300 DPI)



A) The stability of **4e**, **4g** in human and mouse plasma; B) The stability of **4e**, **4g** in human and mouse microsomes (1.0 mg/mL). Vertical bars represent the standard deviation of each data point (n=3).

80x77mm (300 x 300 DPI)



A) Plasma concentration time profile following Intravenous Administration of 20mg/kg **4e**; B) Plasma concentration time profile following Oral Administration of 20 mg/kg **4e**. Each point represents mean  $\pm$  SD (n =3).

80x97mm (300 x 300 DPI)